RESEARCH ARTICLE

Prenatal Exposure to Inflammatory Conditions Increases Cx43 and Panx1 Unopposed Channel Opening and Activation of Astrocytes in the Offspring

Effect on Neuronal Survival

Beatriz C. Avendaño, Trinidad D. Montero, Carolina E. Chávez, Rommy von Bernhardi, and Juan A. Orellana

Several epidemiological studies indicate that children born from mothers exposed to infections during gestation, have an increased risk to develop neurological disorders, including schizophrenia, autism and cerebral palsy. Given that it is unknown if astrocytes and their crosstalk with neurons participate in the above mentioned brain pathologies, the aim of this work was to address if astroglial paracrine signaling mediated by Cx43 and Panx1 unopposed channels could be affected in the offspring of LPS-exposed dams during pregnancy. Ethidium uptake experiments showed that prenatal LPS-exposure increases the activity of astroglial Cx43 and Panx1 unopposed channels in the offspring. Induction of unopposed channel opening by prenatal LPS exposure depended on intracellular Ca^{2+} levels, cytokine production and activation of p38 MAP kinase/iNOS pathway. Biochemical assays and Fura-2AM/DAF-FM time-lapse fluorescence images revealed that astrocytes from the offspring of LPS-exposed dams displayed increased spontaneous Ca^{2+} dynamics and NO production, whereas iNOS levels and release of IL-1β/TNF-α were also increased. Interestingly, we found that prenatal LPS exposure enhanced the release of ATP through astroglial Cx43 and Panx1 unopposed channels in the offspring, resulting in an increased neuronal death mediated by the activation of neuronal $P2X_7$ receptors and Panx1 channels. Altogether, this evidence suggests that astroglial Cx43 and Panx1 unopposed channel opening induced by prenatal LPS exposure depended on the inflammatory activation profile and the activation pattern of astrocytes. The understanding of the mechanism underlying astrocyte-neuron crosstalk could contribute to the development of new strategies to ameliorate the brain abnormalities induced in the offspring by prenatal inflammation.

GLIA 2015;63:2058–2072

Key words: neuroinflammation, hemichannel, connexin, glia, pannexin

Introduction

Different epidemiological studies indicate that children born from mothers exposed to infections during gestation (e.g., sinusitis, pneumonia or pyelonephritis), have an increased risk to develop neurological disorders including schizophrenia, autism and cerebral palsy (Boksa, 2010).These epidemiological data have been supported by a large body of experimental evidence in rodent models mostly based in the administration of lipopolysaccharide (LPS) during pregnancy (Boksa, 2010). Offspring from LPS-exposed pregnant rats exhibit brain cell apoptosis, morphological and structural brain damage, neuronal proliferation deficit, memory and learning impairments and increased anxiety-like behaviors (Golan et al., 2005; Meyer et al., 2006; Rousset et al., 2006). Although it is clear that chronic brain inflammation contributes to the offspring's neurological abnormalities induced by

View this article online at wileyonlinelibrary.com. DOI: 10.1002/glia.22877

Published online June 19, 2015 in Wiley Online Library (wileyonlinelibrary.com). Received Apr 13, 2015, Accepted for publication June 4, 2015.

Address correspondence to Juan A. Orellana, Departamento de Neurología, Escuela de Medicina, Pontificia Universidad Católica de Chile, Marcoleta 391, Santiago, Chile. E-mail: jaorella@uc.cl

From the Departamento de Neurología, Escuela de Medicina, Pontificia Universidad Católica de Chile, Santiago, Chile

prenatal inflammation, involved mechanisms are unknown (Gilmore and Jarskog, 1997).

For a long time, astrocytes were considered to be equivalent to connective tissue or simple support cells in the central nervous system (CNS). However, with the emerging concept of the *tripartite synapse*, astrocytes are now recognized as essential protagonists in brain processing, learning and memory (Araque et al., 2014). To accomplish their regulatory functions on synaptic transmission, most astrocytes express a large repertoire of neurotransmitter receptors, allowing them to sense the neuronal activity and respond locally by the release of "gliotransmitters," such as glutamate, D-serine and ATP (Araque et al., 2014). In addition to their trophic and synaptic role in the CNS, astrocytes are key players in the maintenance of homeostatic balance of pH, neurotransmitters and ions, as well as in the control of cell-to-cell Ca^{2+} signaling and communication (Volterra et al., 2014). The fact that gliotransmitter release by astrocytes could be governed by pro-inflammatory molecules, including cytokines and prostaglandins, indicates that astrocyte-to-neuron signaling could be sensitive to changes in the production of these mediators occurring in pathological conditions (Agulhon et al., 2012). In fact, a CNS inflammatory reaction characterized by astroglial and microglial cell activation has been described in various brain pathologies, including stroke, Alzheimer's disease and meningitis (Verkhratsky et al., 2014). In this process, astrocytes undergo molecular, functional and morphological changes that result in the consequent impairment of the intercellular communication normally occurring among these cells and with neurons (Rossi and Volterra, 2009). Among alterations, changes in intracellular free Ca^{2+} ($[Ca^{2+}]_i$) dynamics, cytokine release and production of nitric oxide (NO) have been reported (Agulhon et al., 2012).

In the CNS, intercellular communication and gliotransmitter release is mediated in part through unopposed plasma membrane channels formed by connexins or pannexins (Montero and Orellana, 2015; Orellana and Stehberg, 2014). These channels, also known as "hemichannels" in the case of those formed by connexins, enable diffusion exchange between the intra- and extracellular compartments under physiological conditions, allowing cellular release of relevant quantities of autocrine/paracrine signaling molecules (MacVicar and Thompson, 2010; Wang et al., 2013b). Nevertheless, it has been proposed that dysregulation of hemichannel and pannexin channel properties could be critical in the genesis and maintenance of homeostatic imbalances observed in several diseases (Bosch and Kielian, 2014; Orellana et al., 2012b; Penuela et al., 2014). Until now, there is no evidence whether glial cell activation and glia-to-neuron communication are affected by prenatal exposure to inflammation. Therefore, our aim was to address if hemichannel and pannexin channel opening and activation of astrocytes was modulated in the offspring from LPS-exposed dams. Here, we show that prenatal LPS exposure induced Cx43 and Panx1 unopposed channel opening in astrocytes by affecting $[Ca^{2+}]_i$ dynamics, cytokine release and NO production. Moreover, Cx43 and Panx1-unopposed channel dependent release of ATP by astrocytes resulted on increased neuronal death by a mechanism involving $P2X_7$ receptors.

Abbreviations

BBG	Brilliant blue G
CNS	Central nervous system
DIV	Days in vitro
DT	Dye transfer
ECL	Enhanced chemiluminescence
FBS	Fetal bovine serum
HBSS	Hank's Balanced Salt Solution
HRP	Horseradish peroxidase
LPS	Lipopolysaccharide
LY	Lucifer yellow
NGS	Normal goat serum
NIH	National Institutes of Health
NO	Nitric oxide
PAGE	Polyacrylamide gel electrophoresis
SDS	Sodium dodecyl sulfate
SL	Scrape-loading

Materials and Methods

Reagents and Antibodies

Gap26, Gap19; TAT-L2 and ^{10}panx1 peptides were obtained from Genscript (New Jersey). HEPES, water (W3500), DMEM, DNAse I, poly-L-lysine, LN-6, A740003, SB203580, MRS2179, polyclonal anti-Cx43 antibody, Anti-GFAP monoclonal antibody, Brilliant blue G (BBG), oATP, Lucifer yellow (LY), ethidium (Etd) bromide, and probenecid (Prob) were purchased from Sigma-Aldrich (St. Louis, MO). Fetal bovine serum (FBS) was obtained from Hyclone (Logan, UT). Penicillin, streptomycin, BAPTA, polyclonal anti-Panx1 antibody (PI488000), FURA-2AM, goat anti-mouse Alexa Fluor 488/555 and goat anti-rabbit Alexa Fluor 488/555 were obtained from Invitrogen (Carlsbad, CA). Anti-NeuN monoclonal antibody and Fluoro-Jade C (F-Jade) were obtained from Chemicon (Martinsried/Munich, Germany). Normal goat serum (NGS) was purchased from Zymed (San Francisco, CA). Anti-Cx43 monoclonal antibody (610061) was obtained from BD Biosciences (Franklin Lakes, NJ). A soluble form of the TNF-α receptor (sTNF-αR1) and a recombinant receptor antagonist for IL-1β (IL-1ra) were from R&D Systems (Minneapolis, MN). Horseradish peroxidase (HRP)-conjugated anti-rabbit IgG was purchased from Pierce (Rockford, IL).

Animals

Animal experimentation was conducted in accordance with the guideline for care and use of experimental animals of the US National Institutes of Health (NIH), guidelines generated by the *ad hoc* committee of the Chilean government (CONICYT) and the Bioethics Committee of the Pontificia Universidad Católica de Chile School of Medicine. Mice of 8–9 weeks of age were housed in cages in a temperature-controlled (24°C) and humidity-controlled

vivarium under a 12 h light/dark cycle (lights on 8:00 AM), with *ad libitum* access to food and water.

Prenatal LPS Exposure Protocol

The protocol of inflammatory stimulation was applied on gestation day 17. Pregnant mice were randomly assigned to one of two groups: (1) control (PBS, i.p injection) and (2) prenatal LPS (0.01 μg/g *E. Coli* LPS, i.p injection). Following full term delivery, offspring were used to prepare astroglial cell primary cultures.

Cell Cultures

Astroglial Cell Cultures. Astroglial cell primary cultures were prepared from cortex of postnatal day 2 (P2) mice as previously described (Orellana et al., 2011b). Briefly, brains were removed, and cortices were dissected. Meninges were carefully peeled off and tissue was mechanically dissociated in Ca^{2+} and Mg^{2+} free Hank's Balanced Salt Solution (CM-HBSS) with 0.25% trypsin and 1% DNase. Cells were seeded onto 60-mm plastic dishes (Nunclon) or onto glass coverslips (Gassalem, Limeil-Brevannes, France) placed inside 16-mm 24-well plastic plates (Nunclon) at the density of $2x10^6$ cells/dish or 1×10^5 cells/well, respectively, in DMEM, supplemented with penicillin (5 U/mL), streptomycin (5 μg/mL), and 10% FBS. After 8–10 days *in vitro* (DIV), 1 μM cytosine-arabinoside was added for 3 days to eliminate proliferating microglia. Medium was changed twice a week and cultures were used after 3 weeks. At that stage, these cultures contained >97% GFAP+ cells. No neurons were detected as judged by MAP2 and NeuN staining.

Neuron Cultures. Neurons were obtained by plating cell suspensions obtained from dissociated E16 mice cerebral cortex ($5x10^4$ cells/coverslip). Briefly, brains were removed, and cortices were dissected. Meninges were carefully peeled off and tissue was mechanically dissociated in CM-HBSS with 0.25% trypsin and gently triturated. Dissociated cells were plated onto poly-D-lysine-coated coverslips in DMEM media with 5% horse serum, 5 U/mL penicillin, and 5 μg/mL streptomycin. After 5 h, medium was replaced with neurobasal medium supplemented with glutamax and B27. After 3 DIV, 1 μM cytosine-arabinoside was added for 3 days to eliminate proliferating astrocytes One fourth of the culture medium was changed twice a week.

Cell Treatments

To obtain conditioned media (CM) from astrocytes, cells were seeded (2×10^6 cells in 35-mm dishes) in DMEM containing 10% FBS for 96 h. Afterwards, CM was collected, filtered (0.22 μm pore), and stored at −20°C until use. Neuronal death was evaluated by F-Jade in neuron cultures exposed to the astrocyte's CM for 3 h with and without co-treatment with blockers of purinergic receptors (oATP, BBG, A740003, MRS2179) and Panx1 hemichannels (^{10}panx1, Prob). To evaluate the involvement of factors released via hemichannels, molecular (siRNAs), and pharmacological (mimetic peptides) inhibition of hemichannels were applied to astroglial cell cultures for 96 h before the CM was collected.

Neuronal Death Quantification

Neuron cultures were fixed in 40% ethanol at 4°C for 5 min, treated with 0.1% Triton X-100 in PBS for 10 min and rinsed twice with distilled water. Preparations were incubated with 0.001% F-Jade in distilled water and gently shaken for 30 min in the dark as described (Schmuck and Kahl, 2009). Later, F-Jade was removed and cells were incubated with anti-NeuN monoclonal antibody (Millipore, 1:500) or anti-MAP2 monoclonal antibody (Sigma, 1:500) diluted in 0.1% PBS-Triton X-100 with 2% NGS at 4°C overnight. After five rinses in 0.1% PBS-Triton X-100, cells were incubated with goat anti-mouse IgG Alexa Fluor 355 (1:1000) at room temperature for 50 min. After several washes, coverslips were mounted in DAKO fluorescent mounting medium and examined with a confocal laser-scanning microscope (Olympus, Fluoview FV1000, Tokyo, Japan).

Dye Uptake and Time-Lapse Fluorescence Imaging

For time-lapse fluorescence imaging, astrocytes plated on glass coverslips were washed twice in HBSS. Then, cells were incubated with Locke's solution with 5 μM Etd. Fluorescence intensity of selected cells was recorded (ROIs, regions of interest) using an Olympus BX 51W1I upright microscope with a 40x water immersion objective. Changes were monitored using an imaging system equipped with a Retga 1300I fast-cooled monochromatic digital camera (12-bit) (Qimaging, Burnaby, BC, Canada), monochromator for fluorophore excitation, and Metafluor software (Universal Imaging, Downingtown, PA) for image acquisition and analysis. To assess for changes in slope, regression lines were fitted to points before and after the various experimental conditions using Excel program, and mean values of slopes were compared using GraphPad Prism software and expressed as AU/min. In some experiments, astrocytes were preincubated with synthetic mimetic peptides, Gap26 (100 μM; VCYDKSFPISHVR, first extracellular loop domain of Cx43), Gap19 (100 μM; KQIEIKKFK, intracellular loop domain of Cx43), TAT-L2 (100 μM; YGRKKRRQRRRDGANVDMHLKQIEIKKF KYGIEEHGK, second intracellular loop domain of Cx43), and ^{10}panx1 (100 μM, WRQAAFVDSY, first extracellular loop domain of Panx1), for 15 min before experiments were performed. Similarly, in another set of experiments, astrocyte cultures were incubated with sTNF-αR1 (soluble form of the receptor that binds TNF-α), IL-1ra (IL-1β receptor endogenous blocker), L-N6 (iNOS inhibitor), or SB203580 (p38 MAP kinase inhibitor) for 24 h.

Scrape Loading/Dye Diffusion Technique

Gap junction permeability was evaluated at room temperature using the scrape-loading/dye transfer (SL/DT) technique. Briefly, astroglial cultures were washed for 10 min in HEPES-buffered salt solution containing the following (in mM): 140 NaCl, 5.5 KCl, 1.8 $CaCl_2$, 1 $MgCl_2$, 5 glucose, 10 HEPES, pH 7.4 followed by washing in a Ca^{2+}-free HEPES solution for 1 min. Then, a razor blade cut was made in the monolayer in a HEPES-buffered salt solution with normal Ca^{2+} concentration containing the fluorescent dye LY. After 1 min, LY (100 μM) was washed out several times with HEPES-buffered salt solution. At five minutes after scraping, fluorescent images were captured using an Olympus BX 51W1I upright microscope with a 40x water immersion objective. Changes were

monitored using an imaging system equipped with a Retga 1300I fast-cooled monochromatic digital camera (12-bit) (Qimaging, Burnaby, BC, Canada), monochromator for fluorophore excitation, and Metafluor software (Universal Imaging, Downingtown, PA) for image acquisition and analysis. For each trial, data were quantified by measuring fluorescence areas in three representative fields. Quantification of changes in gap junctional communication induced by different treatments was performed by measuring the fluorescence area, expressed as arbitrary units (AU).

siRNA Transfection

siRNA duplexes against mouse Cx43 or Panx1 were predesigned and obtained from Origene (Rockville, MD). siRNA (10 nM) was transfected with Oligofectamine (Invitrogen) according to the Origene application guide for Trilencer-27 siRNA. Negligible cell death was detected after transfection (data not shown). Sequences for siRNAs against mouse Cx43 and Panx1 were siRNA-Cx43: rGrCrArGrUrGrCrArCrArUrGrUrArArCrUrArArUrUrUrATT and siRNA-Panx1: rArGrArArCrArUrArArGrUrGrArGrCrUrCrArArArUrCrGTA, respectively.

Immunofluorescence and Confocal Microscopy

Astrocytes grown on coverslips were fixed at room temperature with 2% paraformaldehyde for 30 min and then washed three times with PBS. They were incubated three times for 5 min in 0.1 M PBS-glycine, and then in 0.1% PBS-Triton X-100 containing 10% NGS for 30 min. Cells were incubated with anti-GFAP monoclonal antibody (Sigma, 1:400) and anti-Cx43 polyclonal antibody (SIGMA, 1:400) diluted in 0.1% PBS-Triton X-100 with 2% NGS at 4°C overnight. After five rinses in 0.1% PBS-Triton X-100, cells were incubated with goat anti-mouse IgG Alexa Fluor 355 (1:1000) or goat anti-rabbit IgG Alexa Fluor 488 (1:1000) at room temperature for 50 min. After several rinses, coverslips were mounted in DAKO fluorescent mounting medium and examined with a confocal laser-scanning microscope (Olympus, Fluoview FV1000, Tokyo, Japan).

Intracellular Ca^{2+} and NO Imaging

Cells plated on glass coverslips were loaded with 5 μM Fura-2-AM or 5 μM DAF-FM in DMEM without serum at 37°C for 45 min and then washed three times in Locke's solution (154 mM NaCl, 5.4 mM KCl, 2.3 mM $CaCl_2$, 5 mM HEPES, pH 7.4) followed by de-esterification at 37°C for 15 min. The experimental protocol for $[Ca^{2+}]_i$ and NO imaging involved data acquisition every 5 s (emission at 510 and 515 nm, respectively) at 340/380-nm and 495 excitation wavelengths, respectively, using an Olympus BX 51W1I upright microscope with a 40× water immersion objective. Changes were monitored using an imaging system equipped with a Retga 1300I fast-cooled monochromatic digital camera (12-bit) (Qimaging, Burnaby, BC, Canada), monochromator for fluorophore excitation, and METAFLUOR software (Universal Imaging, Downingtown, PA) for image acquisition and analysis. Analysis involved determination of pixels assigned to each cell. The average pixel value allocated to each cell was obtained with excitation at each wavelength and corrected for background. Due to the low excitation intensity, no bleaching was observed even when cells were illuminated for a few minutes. The FURA-2AM ratio was obtained after dividing the 340-nm by the 380-nm fluorescence image on a pixel-by-pixel base ($R = F_{340\ nm}/F_{380\ nm}$). Fura-2AM *in situ* calibration to obtain the intracellular Ca^{2+} concentration ($[Ca^{2+}]_i$) for single cells was performed according to the equation of Grynkiewicz and colleagues (Grynkiewicz et al., 1985): $[Ca^{2+}]_i = K_d\ \beta(R - R_{min})/(R_{max} - R)$, where $K_d = 224$ nM is the dissociation constant of Fura-2AM and R is the measured F_{340}/F_{380} ratio. The R_{min} was determined by using 10 mM EGTA + 10 μM A23187 in Ca^{2+}-free Locke's solution and R_{max} was obtained by using 5 μM ionomycin and 10 mM $CaCl_2$. β was calculated as the ratio F_{min}/F_{max} at 380 nm.

IL-1β and TNF-α Determination Assay

IL-1β and TNF-α were determined in the astrocyte CM. Samples were centrifuged at 14.000 g for 40 min. Supernatants were collected and protein content assayed by the BCA method. IL-1β and TNF-α levels were determined by sandwich ELISA, according to the manufacturer's protocol (eBioscience, San Diego, CA). For the assay, 100 μL of samples were added *per* ELISA plate well and incubated at 4°C overnight. A calibration curve with recombinant cytokine was included. Detection antibody was incubated at room temperature for 1 h and the reaction developed with avidin–HRP and substrate solution. Absorbance was measured at 450 nm with reference to 570 nm with the microplate reader Synergy HT (Biotek Instruments).

Western Blot Analysis

Astrocytes were rinsed twice with PBS (pH 7.4) and harvested by scraping with a rubber policeman in ice-cold PBS containing 5 mM EDTA, Halt (78440) and M-PER protein extraction cocktail (78501) according to the manufacturer instructions (Pierce, Rockford, IL). The cell suspension was sonicated on ice. Proteins were measured using the Bio-Rad protein assay. Aliquots of cell lysates (100 μg of protein) were resuspended in Laemli's sample buffer, separated in an 8% sodium dodecyl sulfate polyacrylamide gel electrophoresis (SDS-PAGE) and electro-transferred to nitrocellulose sheets. Nonspecific protein binding was blocked by incubation of nitrocellulose sheets in PBS-BLOTTO (5% nonfat milk in PBS) for 30 min. Blots were then incubated with primary antibody at 4°C overnight, followed by four 15 min washes with PBS. Then, blots were incubated with HRP- conjugated goat anti-rabbit antibody at room temperature for 1 h and then rinsed four times with PBS for 15 min. Immunoreactivity was detected by enhanced chemiluminescence (ECL) detection using the SuperSignal kit (Pierce, Rockford, IL) according to the manufactureŕs instructions.

Cell Surface Biotinylation and Quantitation

Cells cultured on 90-mm dishes were washed three times with ice-cold Hank's saline solution (pH 8.0), and 3 mL of sulfo-NHS-SS-biotin solution (0.5 mg/mL) was added followed by incubation for 30 min at 4°C. Cells were washed three times with ice-cold saline containing 15 mM glycine (pH 8.0) to block unreacted biotin. The cells were harvested and incubated with an excess of immobilized NeutrAvidin (1 mL of NeutrAvidin per 3 mg of biotinylated protein) for 1 h at 4°C after which 1 mL of wash buffer (saline solution, pH 7.2 containing 0.1% SDS and 1% Nonidet P-40) was added. The mixture was centrifuged for 2 min at 14.000 r.p.m. at 4°C. The supernatant was removed

and discarded, and the pellet was resuspended in 40 μL of saline solution, pH 2.8 containing 0.1 M glycine, to release the proteins from the biotin. After the mixture was centrifuged at 14,000 r.p.m. at 4°C for 2 min, the supernatant was collected, and the pH was adjusted immediately by adding 10 μL of 1 M Tris, pH 7.5. Relative protein levels were measured using Western blot analysis as described above. Resulting immunoblot signals were scanned, and the densitometric analysis was performed with IMAGEJ software. Densitometric arbitrary units were normalized to the signal obtained from total protein measured with Ponceau red.

Measurement of Extracellular ATP Concentration

ATP concentration was determined in 100 μL of the CM from astrocytes using luciferin/luciferase bioluminescence assay (Sigma-Aldrich). Baseline measurements were performed on separate cultures using standard solutions. The amount of ATP in each sample was calculated from standard curves and normalized for the protein concentration as determined by the BCA assay (Pierce).

Data analysis and Statistics

For each data group, results were expressed as mean ± standard error (SEM); n refers to the number of independent experiments. For statistical analysis, each experimental condition was compared with its corresponding control, and significance was determined using a one-way ANOVA followed, in case of significance, by a Tukey *post-hoc* test.

Results

Astrocytes Obtained From the Offspring of LPS-Exposed Dams Exhibit an Increased Opening of Cx43 and Panx1 Unopposed Channels

It has become increasingly recognized that hemichannels and pannexin channels play a crucial role in the physiology and pathophysiology of the CNS (Montero and Orellana, 2015; Shestopalov and Slepak, 2014). To examine whether astrocytes obtained from the offspring of LPS-exposed dams exhibit an increased hemichannel and pannexin channel activity, the functional state of these channels was assessed by recording the rate of ethidium (Etd) uptake. Etd only crosses the plasma membrane in healthy cells by passing through specific large-pore channels, including hemichannels and pannexin channels. Upon binding to intracellular nucleic acids, Etd becomes fluorescent, indicating channel opening when appropriate blockers are employed (Schalper et al., 2008).

Cultured astrocytes from the offspring of LPS-exposed dams exhibited a ∼3-fold increase in Etd uptake compared with those under control conditions (Fig. 1A–E). Astrocytes express functional hemichannels formed by Cx43 (Contreras et al., 2002) and Panx1 channels (Iglesias et al., 2009). The possible role of Cx43 hemichannels in prenatal LPS exposure-induced Etd uptake was studied using mimetic peptides with sequences homologous to the first extracellular (Gap26) or intracellular (Gap 19 and TAT-L2) loop domains of Cx43 (Wang et al., 2013a). Gap26 (100 μM), Gap19 (100 μM) and TAT-L2 (100 μM) strongly reduced prenatal LPS exposure-induced Etd uptake in astrocytes to ∼126%, ∼177% and ∼137%, respectively (Fig. 1C,D). Supporting these findings, downregulation of Cx43 with $siRNA^{Cx43}$, but not scrambled siRNA completely inhibited the Etd uptake induced by prenatal LPS exposure (Fig. 1D). To scrutinize the involvement of Panx1 channels in the prenatal LPS exposure-induced Etd uptake, we employed a $siRNA^{Panx1}$, probenecid and the mimetic peptide ^{10}panx1 with an amino acid sequence homologous to the first extracellular loop domain of Panx1 (Pelegrin and Surprenant, 2006). Downregulation of Panx1, probenecid (500 μM) and ^{10}panx1 (100 μM) partially inhibited the prenatal LPS exposure-induced Etd uptake in astrocytes (Fig. 1D). These results strongly suggest that prenatal LPS exposure increases the opening of Cx43 and Panx1 unopposed channels in the offspring astrocytes.

Given that previous studies have demonstrated that increased $[Ca^{2+}]_i$, TNF-α/IL-1β release, iNOS/NO and p38 MAPk pathways participate in the opening of glial cell hemichannels (De Bock et al., 2014; Orellana et al., 2013; Retamal et al., 2007), we examined whether these factors were involved in the prenatal LPS exposure-induced unopposed channel activity in astrocytes. BAPTA strongly reduced the prenatal LPS-induced Etd uptake in astrocytes, whereas pretreatment with a soluble form of TNF-α receptor that binds TNF-α (sTNF-aR1) and a recombinant antagonist for IL-1β receptor (IL-1ra) induced similar effects (Fig. 2). When sTNF-aR1 or IL-1ra were applied by themselves, no prevention was observed (Fig. 2). Moreover, the prenatal LPS-induced Etd uptake in astrocytes was robustly blunted by inhibition of p38 MAPk with 10 μM SB202190 or of iNOS by 5 μM L-N6 (Fig. 2). These findings suggest that increased $[Ca^{2+}]_i$, release of TNF-α/IL-1β, and activation of iNOS/p38 MAPk pathways appear to be critical for the opening of astrocyte unopposed channels evoked on the offspring by prenatal LPS exposure.

Prenatal LPS Exposure Increases Surface Levels of Cx43 and Panx1 and Reduces Gap Junctional Communication in Offspring Astrocytes

The increase in unopposed channel activity could be due to an increased opening probability per channel or/and an increase in the number of channels present in the cell membrane. Previous studies have associated hemichannel-mediated dye uptake with increased presence of hemichannels in the astrocyte cell membrane (Orellana et al., 2011a). Therefore, the effect of prenatal LPS exposure on the total and surface levels of Cx43 and Panx1 in offspring's astrocytes was evaluated. Comparable levels of total Cx43 and Panx1 were detected in control astrocytes or those from the offspring of LPS-exposed dams (Fig. 3A,B). However, when compared to control conditions, prenatal LPS exposure induced a ∼2- and ∼8-fold increase of Cx43 and Panx1 present in the cell membrane of offspring's

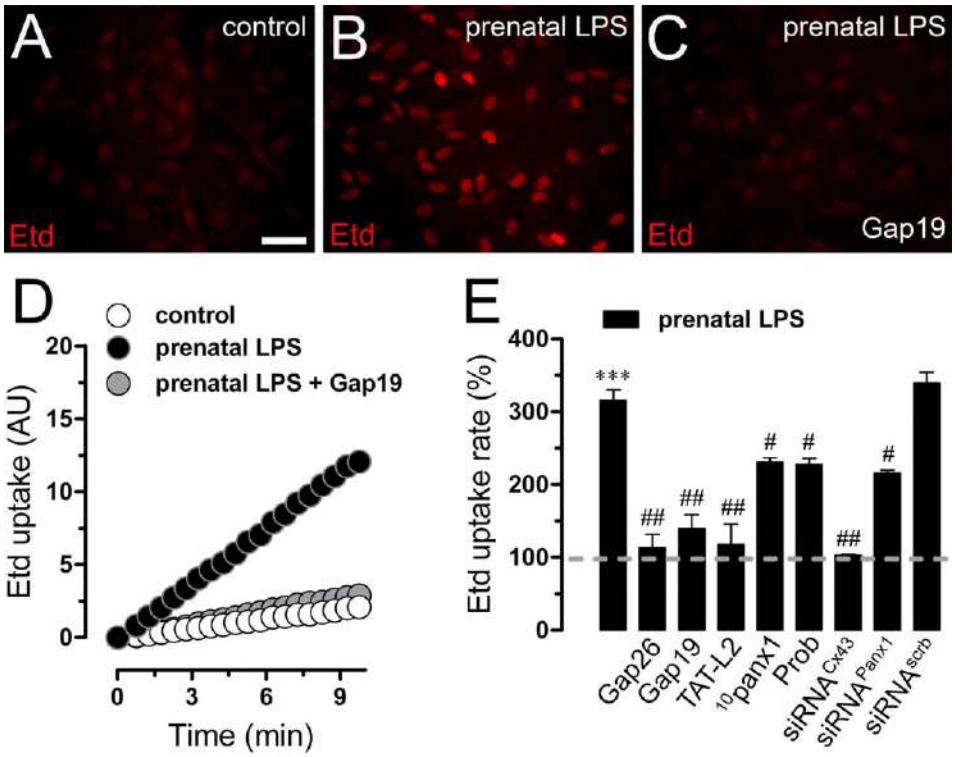

FIGURE 1: Increased Etd uptake induced by prenatal LPS exposure is mediated by Cx43 and Panx1 unopposed channels in offspring's astrocytes. (A–C) Representative fluorescence images depicting nuclear Etd staining (red) in dye uptake experiments (10 min exposure) by astrocytes from offspring of control (A) and LPS-exposed dams alone (B) or with Gap19 (mimetic peptide that blocks Cx43 hemichannels, added during recordings) (C). (D) Time-lapse measurements of Etd uptake by astrocytes from offspring of control (white circles) and LPS-exposed dams alone (black circles) or plus Gap19 added during recordings (gray circles). (E) Averaged Etd uptake rate normalized with control condition (dashed line) by astrocytes from offspring of LPS-exposed dams alone or in combination with the following blockers: 100 μM Gap26, 100 μM Gap19, 100 μM TAT-L2, 100 μM ^{10}panx1, 500 μM Probenecid (Prob), siRNA^{Cx43}, siRNA^{Panx1}; and siRNA^{scrb}. ***$P<0.001$, prenatal LPS protocol compared to control; $^{\#}P<0.05$, $^{\#\#}P<0.005$, effect of prenatal LPS protocol compared to blockers. Data correspond to at least three independent experiments. Scale bar = 100 μm. [Color figure can be viewed in the online issue, which is available at wileyonlinelibrary.com.]

astrocytes, respectively (Fig. 3A–C). These findings support the idea that part of the increased Etd uptake evoked by prenatal LPS exposure in offspring's astrocytes could be linked to an increase of membrane unopposed channels.

In the CNS, gap junctional coupling mediated by Cx43 plays important roles in the propagation of intercellular Ca^{2+} waves, and neurotransmitter and ionic homeostasis, thus helping to ensure proper neuronal function (De Bock et al., 2014). In view of previous studies that have shown that increased hemichannel activity evoked by inflammatory conditions is accompanied with a reduction in dye coupling of astrocytes (Retamal et al., 2007), we investigated whether astroglial cell coupling was affected by prenatal LPS exposure. As previously reported (Giaume et al., 1991; Dermietzel et al., 1991), control astrocytes exhibit a high LY intercellular diffusion (Fig. 4A). However, astrocytes from the offspring of LPS-exposed dams showed a ~50% decrease in LY diffusion when compared with those under control conditions (Fig. 4B,C). Given that retrieval of gap junction channels from the plasma membrane is a mechanism that can lead to cellular uncoupling, we investigated whether LPS exposure-induced astroglial uncoupling was associated with changes in the cell distribution of Cx43. In control astrocytes, Cx43 was detected as fine granules dispersed in cellular interfaces (Fig. 4D,E), whereas in those from offspring of LPS-exposed dams, it was localized mostly at intracellular vesicle-like structures of irregular size, and significantly reduced and disorganized at cell membrane appositions (Fig. 4F,G). These results suggest that cell-to-cell uncoupling evoked by prenatal LPS exposure may be related to a change in the cell distribution of Cx43 in astrocytes.

Astrocytes Obtained From the Offspring of LPS-Exposed Dams Display Enhanced Spontaneous $[Ca^{2+}]_i$ Oscillations

Recent evidence indicate that a moderate rise (>500 nM) of $[Ca^{2+}]_i$ promotes Cx43 hemichannel opening (Wang et al., 2013a), and a similar effect has been described for Panx1 hemichannels (Locovei et al., 2006). Different studies have shown that $[Ca^{2+}]_i$ dynamics play a critical role on astroglial activation, serving as a highly sensitive system to mediate

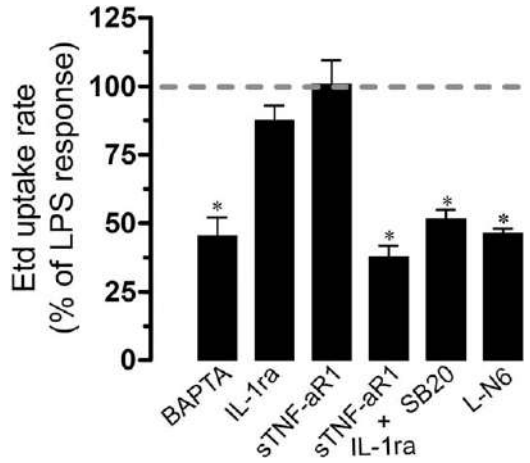

FIGURE 2: Prenatal LPS-induced unopposed channel activity depend on Ca^{2+} signaling, cytokines and activation of p38 MAP kinase/iNOS pathways. Average data normalized to the effect induced by prenatal LPS exposure on Etd uptake rate (dashed line) by astrocytes alone or in co-treatment with the following blockers: 10 μM BAPTA, 100 ng/mL of IL-1ra, 100 ng/mL of sTNF-αR1, 100 ng/mL of IL-1ra + 100 ng/mL of sTNF-αR1, 10 μM SB203580, 1 μM L-N6. *$P < 0.05$, effect of prenatal LPS protocol compared to blockers. Averaged data were obtained from at least three independent experiments.

release of gliotransmitters (Volterra et al., 2014). In fact, astrocytes display spontaneous $[Ca^{2+}]_i$ oscillations that were previously shown to correlate with the release of gliotransmitters regulating local neuronal networks (Volterra et al., 2014). Given that BAPTA strongly reduced prenatal LPS-induced Etd uptake in astrocytes, we evaluated whether this condition could affect $[Ca^{2+}]_i$ levels in offspring's astrocytes. As indicated by the assessment of Fura-2AM ratio (340/380), astrocytes from offspring of LPS-exposed dams showed basal levels of Ca^{2+} signal that were similar to control astrocytes (203.1 ± 9 nM and 221.2 ± 10 nM, respectively, $n = 4$) (Fig. 5A–D). Notably, the percentage of astrocytes that showed oscillatory activity was significantly increased by prenatal LPS exposure (from ~62% to ~89%; $P > 0.05$), when compared with control conditions (Fig. 5E). Moreover, astrocytes from the offspring of LPS-exposed dams exhibited a ~2-fold increase in spontaneous $[Ca^{2+}]_i$ oscillations (Fig. 5F) and displayed higher Ca^{2+} peaks than control astrocytes (Fig. 5F). These results indicate that prenatal LPS exposure affect $[Ca^{2+}]_i$ dynamics in offspring astrocytes, which is probably critical for the opening of astroglial Cx43 hemichannels and Panx1 channels observed under these conditions.

Astrocytes Obtained From the Offspring of LPS-Exposed Dams Exhibit an Increased Release of Inflammatory Cytokines, iNOS Activity and NO Production

Once activated, astrocytes release important amounts of inflammatory cytokines, whose autocrine/paracrine signaling could modulate astroglial properties at the molecular, morphological and functional level (Agulhon et al., 2012; Rossi and Volterra, 2009). Previous studies have shown that IL-1β and TNF-α increase the opening of hemichannels in astrocytes (Froger et al., 2010; Orellana et al., 2011a; Retamal et al., 2007). Because sTNF-aR1 and IL-1ra significantly reduced the prenatal LPS exposure-induced Etd uptake by astrocytes, we evaluated whether these conditions changed the release of IL-1β and TNF-α by astrocytes. Astrocytes from the offspring of LPS-exposed dams exhibited a ~5-fold and ~40-fold increase in the release of IL-1β and TNF-α compared with control conditions, respectively (Fig. 6A). Several of these cytokines regulate astroglial response to pathological conditions by changing NO production (Agulhon et al., 2012). Given that LN-6, a specific iNOS blocker, greatly reduced the prenatal LPS-induced Etd uptake in astrocytes (Fig. 2), we examined if prenatal LPS exposure affected NO production in our experimental model. DAF-FM fluorescence imaging revealed that astrocytes from the offspring of LPS-exposed dams exhibited a ~2-fold increase on basal NO compared with control conditions (Fig. 6C–G). Moreover, prenatal LPS exposure induced a ~2.5-fold increase in iNOS expression (Fig. 6B), suggesting that prenatal LPS-induced NO production in astrocytes could depend on changes in iNOS protein level. Altogether, this evidence indicates that prenatal LPS-induced unopposed channel opening observed

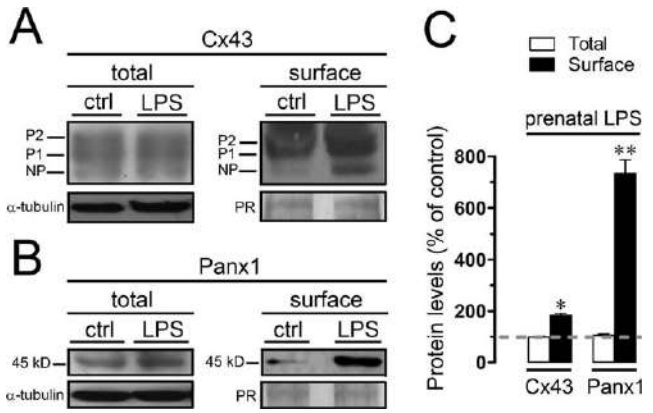

FIGURE 3: Prenatal LPS exposure increases surface levels of Cx43 and Panx1 in offspring astrocytes. Total (left panels) and surface (right panels) levels of Cx43 (A) or Panx1 (B) by astrocytes from offspring of control or LPS-exposed dams. The Cx43 phosphorylated (P1-P2) and nonphosphorylated (NP) forms are indicated in the left. Total levels of each analyzed protein were normalized according to the levels of α-tubulin detected in each lane. Surface levels of each analyzed protein were normalized according to the total protein loaded as revealed by staining with Ponceau red (PR) in each lane. (C) Quantification of total (white bars) and surface (black bars) levels of Cx43 or Panx1 normalized to control (dashed line) in astrocytes from the offspring of LPS-exposed dams. Averaged data were obtained from three independent experiments.

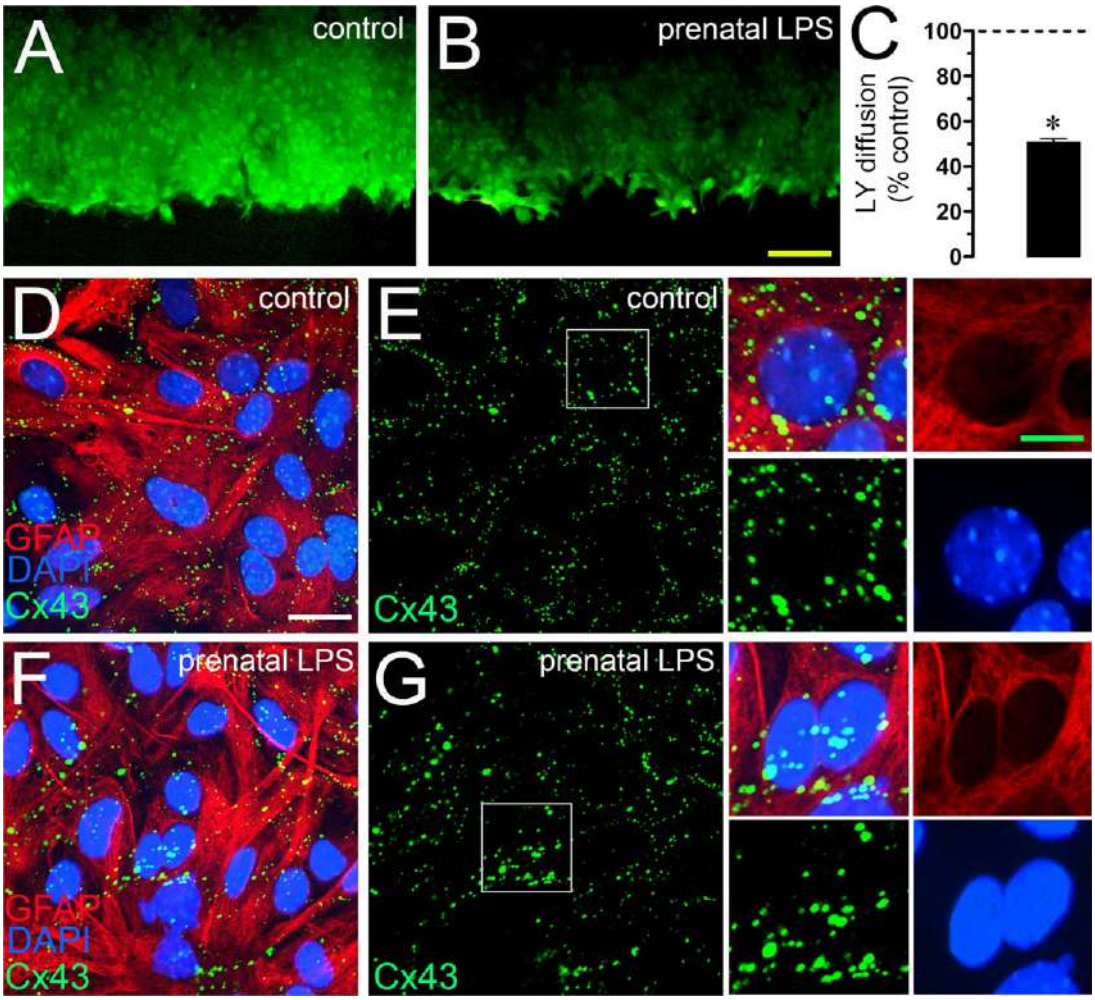

FIGURE 4: Prenatal LPS exposure reduces gap junctional communication and affect cellular distribution of Cx43 in offspring astrocytes. (A–B) Representative fluorescence micrographs of SL/DT with LY by offspring's astrocytes of control (A) or LPS-exposed (B) dams. (C) Averaged data normalized to control (dashed line) of SL/DT with LY by astrocytes from offspring of LPS-exposed dams. * $P < 0.05$, prenatal LPS protocol compared to control. Averaged data were obtained from three independent experiments. Yellow scale bar = 250 μm. (D–G) Representative confocal images depicting Cx43 (green), GFAP (red) and DAPI (blue, epifluorescence) immunolabeling by astrocytes from the offspring of control (D–E) or LPS-exposed (F–G) dams. Insets: 2.5X magnification of the indicated area of panels E and G. Calibration Bars: white = 70 μm and green= 15 μm. [Color figure can be viewed in the online issue, which is available at wileyonlinelibrary.com.]

in astrocytes could be triggered through an autocrine/paracrine effect evoked by inflammatory cytokines and NO.

Prenatal LPS Exposure Induces Cx43 and Panx1-Dependent Release of ATP in Offspring Astrocytes

Astrocytes exposed to inflammatory conditions show an increased hemichannel-dependent release of the gliotransmitter ATP (Orellana et al., 2011a,2011b; Wei et al., 2014). Accordingly, we examined whether prenatal LPS-induced unopposed channel activity observed in astrocytes could be associated with an increased release of ATP. As shown by ATP measurement with the luciferin/luciferase bioluminescence assay, astrocytes from the offspring of LPS-exposed dams exhibited a ~4.5-fold increase on ATP release compared with the control condition (Fig. 7). Gap19 (100 μM) and TAT-L2 (100 μM) abolished the prenatal LPS-induced ATP release in astrocytes (Fig. 7). In agreement with these findings, downregulation of Cx43 by siRNA^{Cx43} completely inhibited the ATP release induced by prenatal LPS exposure (Fig. 7). In addition, the mimetic peptide ^{10}panx1 (100 μM), probenecid (500 μM) and siRNA^{Panx1} partially inhibited prenatal LPS-induced ATP release by astrocytes (Fig. 7). The evidence indicates that prenatal LPS exposure increased the release of ATP by opening of Cx43 and Panx1 unopposed channels in offspring astrocytes.

Recently, it has been demonstrated that ATP elicits its own release in an autocrine manner via P2 receptors and activation of Cx43 and Panx1 unopposed channels (Orellana et al., 2012a; Orellana et al., 2013). We found that 10 μM MRS2179, a $P2Y_1$ receptor blocker, fully abolished the release of ATP induced by prenatal LPS exposure (Fig. 7). The

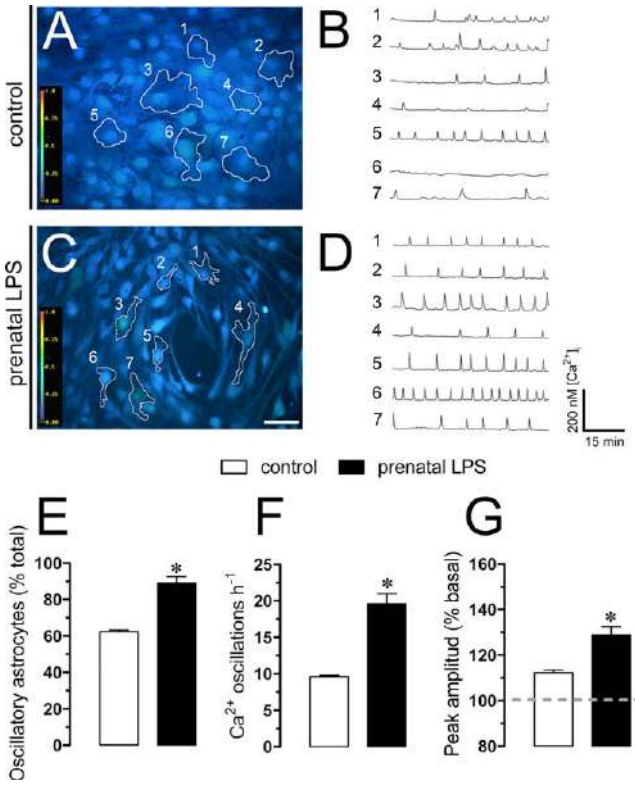

FIGURE 5: Prenatal LPS exposure increases spontaneous Ca^{2+} dynamics by astrocytes from the offspring. (A–D) Representative fluorescence micrographs and plots of basal Fura-2AM ratio (pseudo-colored scale) over time by astrocytes from the offspring of control (A and B) and LPS-exposed dams (C and D). Representative plots of relative changes in $[Ca^{2+}]_i$ over time of cells depicted in panel A and C are shown. (E) Averaged data of the percentage of oscillatory astrocytes from the offspring of control (white bar) and LPS-exposed dams (black bar). (F) Averaged data of oscillation frequency by astrocytes from the offspring of control (white bar) and LPS-exposed dams (black bar). (G) Averaged data of amplitude peak normalized to basal Fura-2AM ratio by astrocytes from the offspring of control (white bar) and LPS-exposed dams (black bar). *$P<0.05$, prenatal LPS protocol compared to control. Averaged data were obtained from at least three independent experiments. Scale bar = 120 μm. [Color figure can be viewed in the online issue, which is available at wileyonlinelibrary.com.]

involvement of $P2X_7$ receptors on the prenatal LPS-induced ATP release was confirmed by the inhibitory effect induced by 200 μM oATP, a general P2X receptor blocker, or 10 μM A740003 and 10 μM BBG, both $P2X_7$ receptor blockers (Fig. 7). These results suggest that activation of both $P2Y_1$ and $P2X_7$ receptors lead to the opening of Cx43 and Panx1 unopposed channels, resulting in further release of ATP.

Astroglial Cx43 and Panx1 Unopposed Channel Opening Induced by Prenatal LPS Exposure Lead to Neuronal Death

Because hemichannel-mediated release of ATP occurs in activated astrocytes, promoting neuronal damage (Orellana et al., 2011a,2011b), we examined whether increased astroglial unopposed channel activity induced by prenatal LPS exposure could affect neurons through a paracrine pathway. Therefore, enriched neuron cultures were incubated for 3 h with conditioned medium (CM) of astrocytes from the offspring of LPS-exposed or control dams. Under control conditions, less than ~2% of 12 day-old MAP-2 and NeuN positive neurons were labeled with F-Jade (Fig. 8A,D,G), a marker of neurodegeneration and neuronal death (Noraberg et al., 1999; Schmuck and Kahl, 2009). After treatment with CM of astrocytes from prenatal LPS-exposed dams, neuronal death showed a 15-fold increase, affecting ~43% of neurons (Fig. 8B,E,G). In contrast, CM of astrocytes from control dams did not affect neuronal survival, supporting the idea that

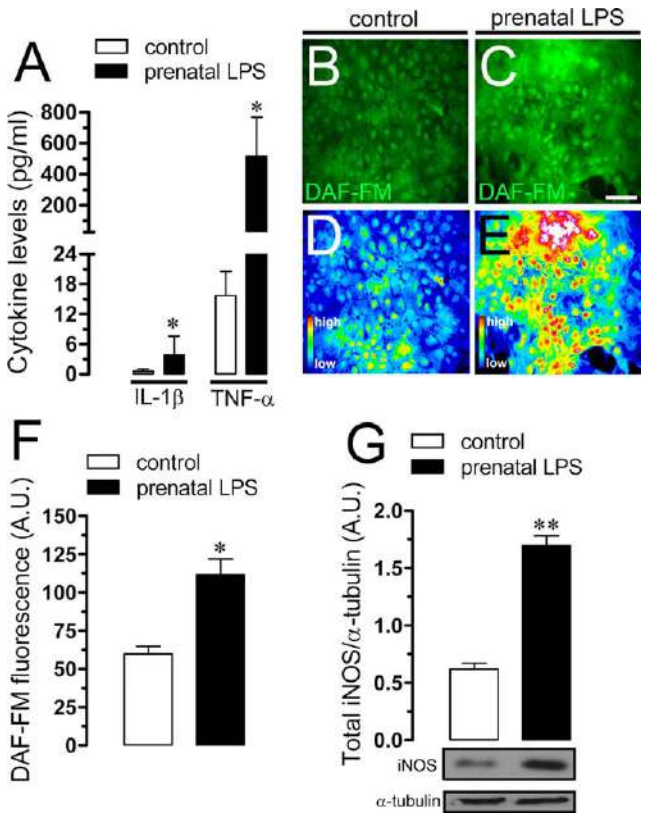

FIGURE 6: Prenatal LPS exposure increases the release of IL-1β and TNF-α and NO production by astrocytes from the offspring. (A) Averaged data of levels of IL-1β and TNF-α released by astrocytes from the offspring of control (white bar) and LPS-exposed dams (black bar). (B–E) Representative fluorescence micrographs of basal NO production (DAF-FM, green and pseudo-colored scale) by astrocytes from the offspring of control (B and D) and LPS-exposed dams (C and E). (F) Average of DAF-FM fluorescence by astrocytes from the offspring of control (white bar) and LPS-exposed dams (black bar). (G) Quantification of protein level of iNOS by astrocytes from the offspring of control (white bar, lane1) and LPS-exposed dams (black bar, lane 2). Protein expression was normalized by the corresponding level of α-tubulin. *$P<0.05$, **$P<0.005$; prenatal LPS protocol compared to control. Averaged data were obtained from at least three independent experiments. Scale bar = 150 μm. [Color figure can be viewed in the online issue, which is available at wileyonlinelibrary.com.]

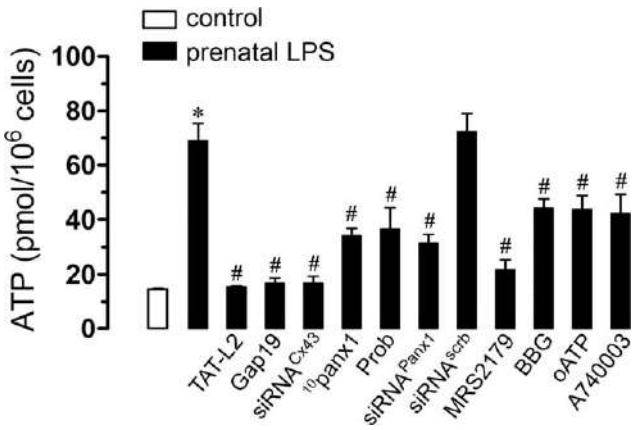

FIGURE 7: Prenatal LPS exposure increases the unopposed channel-dependent release of ATP by astrocytes from the offspring. Averaged data of ATP release by astrocytes from the offspring of control (white bar) and LPS-exposed dams alone (black bars) or in combination with the following blockers: 100 μM TAT-L2, 100 μM Gap19, siRNA^{Cx43}, 100 μM ^{10}panx1, 500 μM Probenecid (Prob), siRNA^{Panx1}; and siRNA^{scrb}, 10 μM MRS2179, 10 μM (BBG), 200 μM oxidized ATP (oATP) and 10 μM A740003. * $P<0.05$, prenatal LPS protocol compared to control; # $P<0.05$; ## $P<0.005$, effect of prenatal LPS protocol compared to blockers. Averaged data were obtained from at least three independent experiments.

prenatal LPS-exposure could potentiate neurotoxic activation of astrocytes (Fig. 8G). Neuronal death was associated with focal beadlike swellings of dendrites and axons (neuritic beading), which has been proposed as an early pathological feature of neuronal cell dysfunction (Fig. 8B) (Takeuchi et al., 2005). To elucidate the contribution of ATP released from astrocytes in the CM-induced neuronal death, we employed blockers of $P2Y_1$ (MRS2179) and $P2X_7$ receptors (BBG, oATP, A740003). MRS2179 (10 μM) failed on inhibiting CM-induced neuronal death (Fig. 8G), whereas BBG (10 μM), oATP (200 μM) and A740003 (10 μM) abolished neurotoxicity, reducing neuronal death from ∼43% to ∼2% in all cases (Fig. 8C,F,G). These findings imply that ATP released by astrocytes into the CM and its action on neuronal $P2X_7$ receptors is part of the mechanism that decrease neuronal survival in our experimental model. Because activation of neuronal purinergic receptors and further activation of Panx1 channels lead to neuronal death (Orellana et al., 2011a,2011b), we inhibited neuronal Panx1 channels with ^{10}panx1 and probenecid to examine their contribution to the CM-induced neuronal death. ^{10}panx1 and probenecid also abolished CM-induced neuronal death (F-Jade+ cells were reduced from ∼43% to ∼2%, Fig. 8G), indicating that ATP released from astrocytes acted on $P2X_7$ receptor and induced further opening of neuronal Panx1 channels. Notably, when CM were obtained from astrocytes exposed to TAT-L2 or Gap19, the induction of neuronal death was abolished (Fig. 8G). Similar findings were obtained in neurons treated with CM from siRNA^{Cx43}-treated astrocytes (Fig. 8G), whereas only a partial reduction in death was observed with CM from astrocytes treated with ^{10}panx1, probenecid or siRNA^{Panx1} (from ∼43% to ∼15%, ∼14% and ∼14.5%, respectively) (Fig. 8G). The above data suggest that unopposed channel opening and neuronal death was due to the Cx43 and Panx1-dependent release of ATP by astrocytes obtained from the offspring of LPS-exposed dams.

Discussion

Despite that previous studies have demonstrated that prenatal inflammation increases astrogliosis and GFAP expression in the offspring (Hao et al., 2010; Samuelsson et al., 2006), whether astrocytes contribute to brain dysfunction induced by the latter condition has remained unknown (Gilmore and Jarskog, 1997). Our model, consisting in a single LPS injection during pregnancy, increased the production of inflammatory mediators (cytokines and NO) and altered intracellular Ca^{2+} dynamics in offspring astrocytes. Due to these functional changes, astrocytes exhibited an enhanced p38MAPK/iNOS-dependent release of ATP via astroglial cell Cx43 and Panx1 unopposed channels, which in consequence caused the impairment of neuronal survival.

As assayed by Etd uptake experiments, prenatal LPS-induced unopposed channel activity was due to Cx43 and Panx1, since it did not occur when astrocytes were treated with siRNAs that downregulated both proteins. Second, drugs and mimetic peptides known to block Cx43 or Panx1 unopposed channels significantly inhibited the above response. How does LPS exposure induce the opening of Cx43 and Panx1 unopposed channels in astrocytes? It is broadly known that maternal environment and physiological status during pregnancy could be crucial in the inflammatory balance and immunity response in the offspring (Boksa, 2010). At one end, prenatal LPS-induced inflammatory conditions may lead to a long-lasting activation of glial cells and thereof a long-term production of inflammatory mediators, including IL-1β and TNF-α (Fig. 9). Indeed, both cytokines are upregulated in the offspring's brain of LPS-exposed dams (Boksa, 2010) and their production has been involved in the opening of astroglial hemichannels (Retamal et al., 2007). Supporting this evidence, we found that prenatal LPS exposure increases the astroglial production of IL-1β and TNF-α, whereas inhibition of IL-1β/TNF-α signaling significantly blunted the prenatal LPS-induced unopposed channel opening in offspring astrocytes. These inflammatory cytokines likely triggered by a p38 MAPk/iNOS-dependent S-nitrosylation of Cx43, resulting in further opening of astroglial hemichannels, as has been previously described (Froger et al., 2010; Orellana et al., 2011a; Retamal et al., 2006, 2007) (Fig. 9). In agreement with this idea, we observed that prenatal LPS-induced

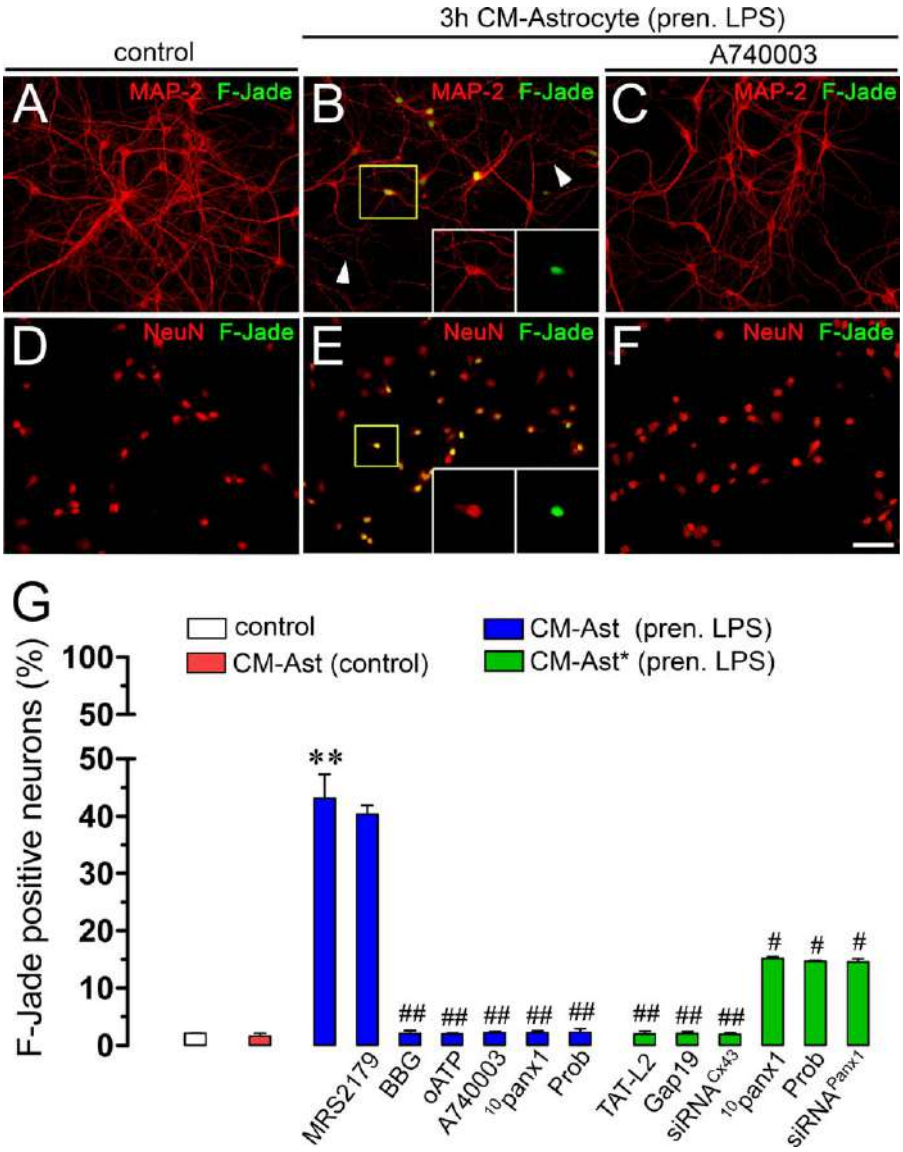

FIGURE 8: Prenatal LPS-induced release of ATP via astroglial Cx43 and Panx1 unopposed channels trigger neuronal death by activation of neuronal $P2X_7$ receptors and Panx1 channels. (A–F) Representative immunofluorescence images depicting MAP-2 (red), NeuN (red) or F-Jade (green) labeling of neurons under control conditions (A and D), treated for 3 h with CM harvested from astrocytes (CM-Ast) of prenatal LPS protocol alone (B and E) or with CM-Ast of prenatal LPS protocol plus 10 μM A740003 (C and F). The respective bottom insets of representative with staining for MAP2, NeuN and F-Jade are also shown in B and E. (G) Averaged data of neuronal death as percent of neurons positive to F-Jade staining under control conditions (white bar), treated for 3 h with CM-Ast of control conditions (red bar) or prenatal LPS protocol alone (blue bars) or in combination with the following blockers: 10 μM MRS2179, 10 μM (BBG), 200 μM oxidized ATP (oATP), 10 μM A740003, 100 μM ^{10}panx1, 500 μM Probenecid. In some experiments, the effect on neuronal death of CM-Ast of prenatal LPS protocol made in the presence of 100 μM TAT-L2, 100 μM Gap19, siRNA^{Cx43}, 100 μM ^{10}panx1, 500 μM Probenecid (Prob), or siRNA^{Panx1} was studied (*, green bars). $^{**}P < 0.005$, CM-Ast of prenatal LPS protocol compared to control; $^{\#}P < 0.05$; $^{\#\#}P < 0.005$, effect of CM-Ast prenatal LPS protocol compared to blockers. Averaged data were obtained from at least three independent experiments. Scale bar = 150 μm. [Color figure can be viewed in the online issue, which is available at wileyonlinelibrary.com.]

astroglial Etd uptake was strongly reduced by inhibiting p38 MAPk or iNOS. Moreover, prenatal LPS exposure increased protein levels of iNOS and NO production in offspring astrocytes, revealing their activated state. Given that S-nitrosylation inhibits the opening of Panx1 channels (Lohman et al., 2012), their activation possibly took place by a different manner.

How does unopposed channel opening evoked by prenatal LPS exposure affect intercellular communication among astrocytes? ATP is considered to be an essential transmitter for the communication among astrocytes, and can be released through membrane channels and vesicles (Fields and Burnstock, 2006). Here, we demonstrated that prenatal LPS exposure triggered the release of ATP from astrocytes via Cx43

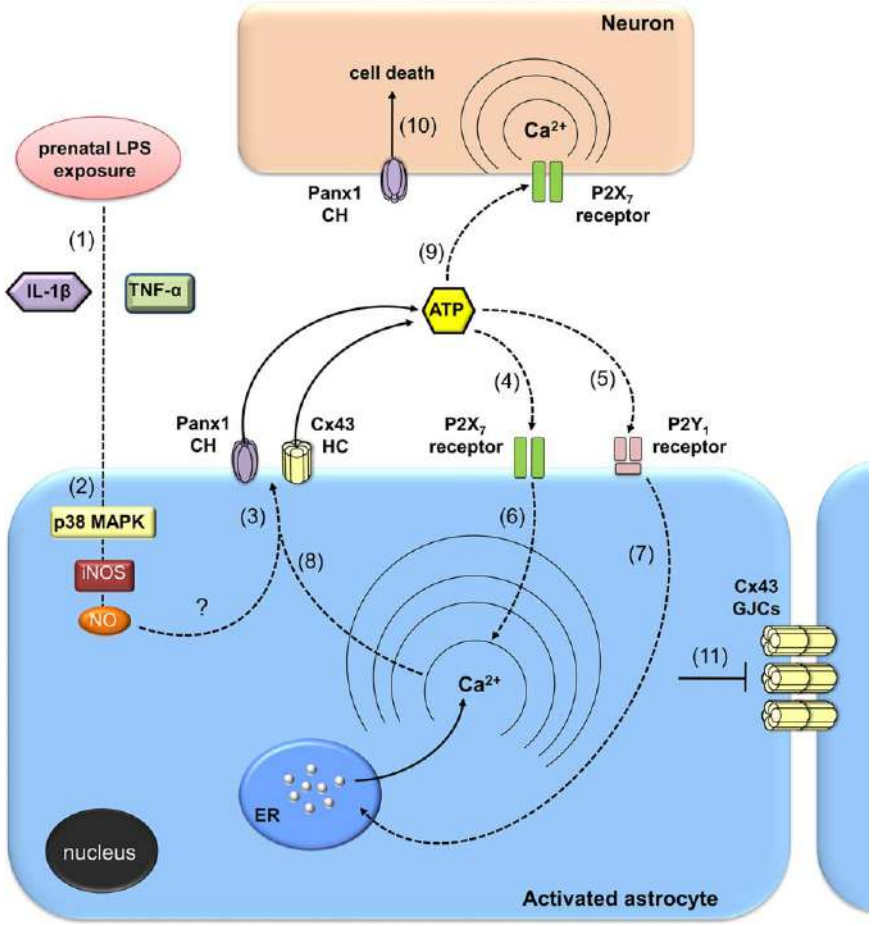

FIGURE 9: Modulation of astroglial Cx43 hemichannels and Panx1 channels by prenatal LPS exposure. Prenatal LPS exposure increase the release of IL-1β and TNF-α in astrocytes (1), leading to the activation of a p38MAPK/iNOS-dependent pathway and further production of NO (2). By an unknown mechanism NO evoke the activation of Cx43 and/or Panx1 unopposed channels (3). ATP released via unopposed channels activates $P2X_7$ and $P2Y_1$ receptors (4 and 5), triggering a self-perpetuating mechanism, in which high levels of $[Ca^{2+}]_i$ (6 and 7) could reactivate Cx43 and Panx1 unopposed channels in astrocytes (8). In addition, paracrine release of ATP from astrocytes could act on neighboring or distant neurons, resulting in the activation of $P2X_7$ (9) receptors. The latter increase levels of $[Ca^{2+}]_i$, and thereof the activity of neuronal Panx1 channels (10), resulting in neuronal function impairment and cell death. Contrary to the effect on unopposed channel function, prenatal LPS exposure additionally decreased the functional coupling between offspring astrocytes (11). [Color figure can be viewed in the online issue, which is available at wileyonlinelibrary.com.]

and Panx1 unopposed channels and depended on $P2Y_1$ and $P2X_7$ receptors (Fig. 9). In fact, prenatal LPS exposure-induced ATP release was not detected after pharmacological (e.g., drugs, mimetic peptides) or molecular (siRNAs) inhibition of Cx43/Panx1 unopposed channels and $P2Y_1$/$P2X_7$ receptors. In agreement with our observations, recent reports have shown that ATP induces its own release via hemichannels and subsequent activation of purinergic receptors (Orellana et al., 2012a; Orellana et al., 2013). In our system, autocrine/paracrine release of ATP could control unopposed channel opening as a secondary mechanism to that exerted by p38 MAPk and NO production (Fig. 9). The opening of unopposed channels could take place by protein–protein interactions with activated $P2X_7$ receptors (Iglesias et al., 2008) or through increases in $[Ca^{2+}]_i$ caused by activation of $P2Y_1$ receptors (Locovei et al., 2006; Orellana et al., 2012a; Saez et al., 2013). Indeed, previous studies have shown that a moderate rise in $[Ca^{2+}]_i$ (>500 nM) evokes Cx43 (Wang et al., 2013a), as well as Panx1 (Locovei et al., 2006) unopposed channel opening. In line with the latter, we observed that chelation of $[Ca^{2+}]_i$ blunted the prenatal LPS-induced unopposed channel opening in offspring astrocytes. Previous evidence indicates that rises on $[Ca^{2+}]_i$ increases levels of surface Cx43 hemichannels, enhancing their contribution to the release of paracrine mediators (Schalper et al., 2008). Relevant to this point, we found that prenatal LPS exposure increased the amplitude and number of spontaneous $[Ca^{2+}]_i$ oscillations in astrocytes, which could explain the increased levels of surface Cx43 and Panx1 unopposed channels observed under these conditions. Impaired transmission of

intercellular Ca^{2+} waves and change of Ca^{2+} dynamics often have been related with altered gliotransmission evoked by inflammatory conditions in astrocytes (Agulhon et al., 2012). Part of this communication is mediated by cell-to-cell coupling mediated by gap junction channels. Here, we observed that in addition to increase unopposed channel opening, prenatal LPS exposure also reduced astroglial coupling as measured by LY diffusion. These data are in agreement with the proposed idea that hemichannels and gap junction channels are oppositely regulated during inflammatory conditions (Orellana et al., 2009). Nevertheless, this phenomenon often lacks correlate between *in vivo* and *ex vivo* models, as previously shown for the opposite regulation of astroglial hemichannels and gap junction channels induced by LPS-stimulated microglia (Retamal et al., 2007; Abudara et al., 2015). Whether this could be also the case in our experimental model is unknown and thereof, further studies are required to elucidate the biological relevance of this phenomenon and the possible impact of other cell types (e.g., neurons) *in vivo*.

How does unopposed channel opening evoked by prenatal LPS exposure affect astrocyte-neuron crosstalk? Having described that CM harvested from activated astrocytes reduces neuronal survival by activating Panx1 channels and $P2X_7$ receptors in neurons (Orellana et al., 2011a; Orellana et al., 2011b); here, we show that ATP released through Cx43 and Panx1 unopposed channels activated $P2X_7$ receptors and Panx1 channels in neurons, increasing neuronal death. Since activation of $P2X_7$ receptors lead to opening of Panx1 channels (Iglesias et al., 2008), it is plausible that CM-induced neuronal death could be associated with an ionic, osmotic and intracellular Ca^{2+} imbalance evoked by $P2X_7$ receptor and Panx1 channel activation. We propose that ATP released from astrocytes could stimulate distant astrocytes and neurons in a paracrine manner, causing Ca^{2+} responses that could depend on the inflammatory profile of astrocytes (Fig. 9). If that is correct, the activation of purinergic receptors could be turned off in part by diffusion of ATP to distal regions as well as by desensitization of $P2Y_1$ receptors and degradation of extracellular ATP by exonucleases. In parallel, an alternative negative feedback loop is the inhibitory effect that could be exerted by ATP on Panx1 channels (Qiu and Dahl, 2009). Alternatively, we cannot rule out that astroglial hemichannel-dependent neuronal death *in vivo*, could occurs in addition with other direct effects evoked by astrocytes (e.g., high release of cytokines) that impact neuronal survival (Boksa, 2010).

Whereas hemichannel and pannexin channel-dependent release of gliotransmitters underlies crucial functions in the physiology of the CNS (Montero and Orellana, 2015; Orellana and Stehberg, 2014), their uncontrolled opening could lead to excitotoxicity (Orellana et al., 2011a,2011b; Takeuchi et al., 2006). Here, we showed for the first time that prenatal LPS exposure increases Cx43 and Panx1 unopposed channel opening in the offspring's astrocytes. These findings are in agreement with recent reports showing that pro-inflammatory conditions increase the opening of astroglial Cx43 hemichannels (Orellana et al., 2011b; Orellana et al., 2014b; Retamal et al., 2007). In addition, although previous studies have found that LPS indirectly open Cx43 hemichannels but not Panx1 channels in astrocytes (Abudara et al., 2015; Retamal et al., 2007), this study, in agreement with recent reports (Beckel et al., 2014; Iwabuchi and Kawahara, 2011; Pan et al., 2015; Santiago et al., 2011; Wei et al., 2014), reveals that Panx1 can form functional channels in these cells. Additional studies will be required to determine whether inflammatory profile of astrocytes and activity of their unopposed channels could determine neuronal survival *in vivo*. Understanding of the mechanisms underlying astrocyte-neuron crosstalk can contribute to the knowledge on the pathways implicated on neuroinflammation and open novel therapeutic avenues for ameliorate the brain abnormalities induced by prenatal inflammation in the offspring.

Acknowledgment

Grant sponsor: FONDECYT 11121133 (to J.A.O.), the Committee for Aid and Education in Neurochemistry from the International Society for Neurochemistry (to J.A.O.) and FONDECYT 1131025 (to R.v.B.).

References

Abudara V, Roux L, Dallérac G, Matias I, Dulong J, Mothet JP, Rouach N, Giaume C. 2015. Activated microglia impairs neuroglial interaction by opening Cx43 hemichannels in hippocampal astrocytes. Glia 63:795–811.

Agulhon C, Sun MY Murphy T, Myers T, Lauderdale K Fiacco TA. 2012. Calcium Signaling and Gliotransmission in Normal vs. Reactive Astrocytes. Front Pharmacol 3:139–

Araque A, Carmignoto G, Haydon PG, Oliet SH, Robitaille R, Volterra A. 2014. Gliotransmitters travel in time and space. Neuron 81:728–739.

Beckel JM, Argall AJ, Lim JC, Xia J, Lu W, Coffey EE, Macarak EJ, Shahidullah M, Delamere NA Zode GS, et al. 2014. Mechanosensitive release of adenosine 5′-triphosphate through pannexin channels and mechanosensitive upregulation of pannexin channels in optic nerve head astrocytes: A mechanism for purinergic involvement in chronic strain. Glia 62: 1486–1501.

Boksa P. 2010. Effects of prenatal infection on brain development and behavior: A review of findings from animal models. Brain Behav Immun 24: 881–897.

Bosch M, Kielian T. 2014. Hemichannels in neurodegenerative diseases: Is there a link to pathology? Front Cell Neurosci 8:242-

Contreras JE, Sánchez HA, Eugenin EA, Speidel D, Theis M, Willecke K, Bukauskas FF, Bennett MVL, Sáez JC. 2002. Metabolic inhibition induces opening of unapposed connexin 43 gap junction hemichannels and reduces gap junctional communication in cortical astrocytes in culture. Proc Natl Acad Sci U S A 99:495–500.

De Bock M, Decrock E, Wang N, Bol M, Vinken M, Bultynck G, Leybaert L. 2014. The dual face of connexin-based astroglial Ca(2+) communication: A key player in brain physiology and a prime target in pathology. Biochim Biophys Acta 1843:2211–2232.

Dermietzel R, Hertberg EL, Kessler JA Spray DC. 1991. Gap junctions between cultured astrocytes: Immunocytochemical, molecular, and electrophysiological analysis. J Neurosci 11:1421–1432.

Fields RD, Burnstock G. 2006. Purinergic signalling in neuron-glia interactions. Nat Rev Neurosci 7:423–436.

Froger N, Orellana JA, Calvo CF, Amigou E, Kozoriz MG, Naus CC, Saez JC, Giaume C. 2010. Inhibition of cytokine-induced connexin43 hemichannel activity in astrocytes is neuroprotective. Mol Cell Neurosci 45:37–46.

Giaume C, Fromaget C, el Aoumari A, Cordier J, Glowinski J, Gros D. 1991. Gap junctions in cultured astrocytes: Single-channel currents and characterization of channel-forming protein. Neuron 6:133–143.

Gilmore JH, Jarskog LF. 1997. Exposure to infection and brain development: Cytokines in the pathogenesis of schizophrenia. Schizophr Res 24:365–367.

Golan HM, Lev V, Hallak M, Sorokin Y, Huleihel M. 2005. Specific neurodevelopmental damage in mice offspring following maternal inflammation during pregnancy. Neuropharmacology 48:903–917.

Grynkiewicz G, Poenie M, Tsien RY. 1985. A new generation of Ca2+ indicators with greatly improved fluorescence properties. J Biol Chem 260: 3440–3450.

Hao LY, Hao XQ, Li SH, Li XH. 2010. Prenatal exposure to lipopolysaccharide results in cognitive deficits in age-increasing offspring rats. Neuroscience 166:763–770.

Iglesias R, Dahl G, Qiu F, Spray DC, Scemes E. 2009. Pannexin 1: The molecular substrate of astrocyte "hemichannels". J Neurosci 29:7092–7097.

Iglesias R, Locovei S, Roque A, Alberto AP, Dahl G, Spray DC, Scemes E. 2008. P2X7 receptor-Pannexin1 complex: Pharmacology and signaling. Am J Physiol Cell Physiol 295:C752–C760.

Iwabuchi S, Kawahara K. 2011. Functional significance of the negative-feedback regulation of ATP release via pannexin-1 hemichannels under ischemic stress in astrocytes. Neurochem Int 58:376–384.

Locovei S, Wang J, Dahl G. 2006. Activation of pannexin 1 channels by ATP through P2Y receptors and by cytoplasmic calcium. FEBS Lett 580:239–244.

Lohman AW, Weaver JL, Billaud M, Sandilos JK, Griffiths R, Straub AC, Penuela S, Leitinger N, Laird DW Bayliss DA, et al. 2012. S-nitrosylation inhibits pannexin 1 channel function. J Biol Chem 287:39602–39612.

MacVicar BA, Thompson RJ. 2010. Non-junction functions of pannexin-1 channels. Trend Neurosci 33:93–102.

Meyer U, Nyffeler M, Engler A, Urwyler A, Schedlowski M, Knuesel I, Yee BK, Feldon J. 2006. The time of prenatal immune challenge determines the specificity of inflammation-mediated brain and behavioral pathology. J Neurosci 26:4752–4762.

Montero TD, Orellana JA. 2015. Hemichannels: New pathways for gliotransmitter release. Neuroscience 286C:45–59.

Noraberg J, Kristensen BW, Zimmer J. 1999. Markers for neuronal degeneration in organotypic slice cultures. Brain Res Brain Res Protoc 3:278–290.

Orellana JA, Busso D, Ramirez G, Campos M, Rigotti A, Eugenin J, von Bernhardi R. 2014a. Prenatal nicotine exposure enhances Cx43 and Panx1 unopposed channel activity in brain cells of adult offspring mice fed a high-fat/cholesterol diet. Front Cell Neurosci 8:403-

Orellana JA, Froger N, Ezan P, Jiang JX, Bennett MV, Naus CC, Giaume C, Saez JC. 2011a. ATP and glutamate released via astroglial connexin 43 hemichannels mediate neuronal death through activation of pannexin 1 hemichannels. J Neurochem 118:826–840.

Orellana JA, Montero TD, von Bernhardi R. 2013. Astrocytes inhibit nitric oxide-dependent Ca(2+) dynamics in activated microglia: Involvement of ATP released via pannexin 1 channels. Glia 61:2023–2037.

Orellana JA, Saez JC, Bennett MV, Berman JW, Morgello S, Eugenin EA. 2014b. HIV increases the release of dickkopf-1 protein from human astrocytes by a Cx43 hemichannel-dependent mechanism. J Neurochem 128:752–763.

Orellana JA, Sáez PJ, Cortés-campos C, Elizondo RJ, Shoji KF, Contreras-Duarte S, Figueroa V, Velarde V, Jiang JX Nualart F, et al. 2012a. Glucose increases intracellular free Ca(2+) in tanycytes via ATP released through connexin 43 hemichannels. Glia 60:53–68.

Orellana JA, Sáez PJ, Shoji KF, Schalper KA, Palacios-Prado N, Velarde V, Giaume C, Bennett MV, Sáez JC. 2009. Modulation of brain hemichannels and gap junction channels by pro-inflammatory agents and their possible role in neurodegeneration. Antioxid Redox Signal 11:369–399.

Orellana JA, Shoji KF, Abudara V, Ezan P, Amigou E, Saez PJ, Jiang JX, Naus CC, Saez JC, Giaume C. 2011b. Amyloid beta-induced death in neurons involves glial and neuronal hemichannels. J Neurosci 31:4962–4977.

Orellana JA, Stehberg J. 2014. Hemichannels: New roles in astroglial function. Front Physiol 5:193-

Orellana JA, von Bernhardi R, Giaume C, Saez JC. 2012b. Glial hemichannels and their involvement in aging and neurodegenerative diseases. Rev Neurosci 23:163–177.

Pan HC, Chou YC, Sun SH. 2015. P2X7 R-mediated Ca(2+) -independent d-serine release via pannexin-1 of the P2X7 R-pannexin-1 complex in astrocytes. Glia 63:877–893.

Pelegrin P, Surprenant A. 2006. Pannexin-1 mediates large pore formation and interleukin-1beta release by the ATP-gated P2X7 receptor. EMBO J 25: 5071–5082.

Penuela S, Harland L, Simek J, Laird DW. 2014. Pannexin channels and their links to human disease. Biochem J 461:371–381.

Qiu F, Dahl G. 2009. A permeant regulating its permeation pore: Inhibition of pannexin 1 channels by ATP. Am J Physiol Cell Physiol 296:C250–C255.

Retamal MA, Cortes CJ, Reuss L, Bennett MV, Saez JC. 2006. S-nitrosylation and permeation through connexin 43 hemichannels in astrocytes: Induction by oxidant stress and reversal by reducing agents. Proc Natl Acad Sci U S A 103:4475–4480.

Retamal MA, Froger N, Palacios-Prado N, Ezan P, Saez PJ, Saez JC, Giaume C. 2007. Cx43 hemichannels and gap junction channels in astrocytes are regulated oppositely by proinflammatory cytokines released from activated microglia. J Neurosci 27:13781–13792.

Rossi D, Volterra A. 2009. Astrocytic dysfunction: Insights on the role in neurodegeneration. Brain Res Bull 80:224–232.

Rousset CI, Chalon S, Cantagrel S, Bodard S, Andres C, Gressens P, Saliba E. 2006. Maternal exposure to LPS induces hypomyelination in the internal capsule and programmed cell death in the deep gray matter in newborn rats. Pediatr Res 59:428–433.

Saez PJ, Shoji KF, Retamal MA, Harcha PA, Ramirez G, Jiang JX, von Bernhardi R, Saez JC. 2013. ATP is required and advances cytokine-induced gap junction formation in microglia in vitro. Mediators Inflamm 2013:216402-

Santiago MF, Veliskova J, Patel NK, Lutz SE, Caille D, Charollais A, Meda P, Scemes E. 2011. Targeting pannexin1 improves seizure outcome. PLoS One 6:e25178-

Samuelsson AM, Jennische E, Hansson HA Holmang A. 2006. Prenatal exposure to interleukin-6 results in inflammatory neurodegeneration in hippocampus with NMDA/GABA(A) dysregulation and impaired spatial learning. Am J Physiol Regul Integr Comp Physiol 290:R1345–R1356.

Schalper KA, Palacios-Prado N, Orellana JA, Saez JC. 2008. Currently used methods for identification and characterization of hemichannels. Cell Commun Adhes 15:207–218.

Schmuck G, Kahl R. 2009. The use of Fluoro-Jade in primary neuronal cell cultures. Arch Toxicol 83:397–403.

Shestopalov VI, Slepak VZ. 2014. Molecular pathways of pannexin1-mediated neurotoxicity. Front Physiol 5:23-

Takeuchi H, Jin S, Wang J, Zhang G, Kawanokuchi J, Kuno R, Sonobe Y, Mizuno T, Suzumura A. 2006. Tumor necrosis factor-alpha induces

neurotoxicity via glutamate release from hemichannels of activated microglia in an autocrine manner. J Biol Chem 281:21362–21368.

Takeuchi H, Mizuno T, Zhang G, Wang J, Kawanokuchi J, Kuno R, Suzumura A. 2005. Neuritic beading induced by activated microglia is an early feature of neuronal dysfunction toward neuronal death by inhibition of mitochondrial respiration and axonal transport. J Biol Chem 280:10444–10454.

Verkhratsky A, Parpura V, Pekna M, Pekny M, Sofroniew M. 2014. Glia in the pathogenesis of neurodegenerative diseases. Biochem Soc Trans 42:1291–1301.

Volterra A, Liaudet N, Savtchouk I. 2014. Astrocyte Ca(2)(+) signalling: An unexpected complexity. Nat Rev Neurosci 15:327–335.

Wang N, De Bock M, Decrock E, Bol M, Gadicherla A, Bultynck G, Leybaert L. 2013a. Connexin targeting peptides as inhibitors of voltage- and intracellular Ca2+-triggered Cx43 hemichannel opening. Neuropharmacology 75:506–516.

Wang N, De Bock M, Decrock E, Bol M, Gadicherla A, Vinken M, Rogiers V, Bukauskas FF, Bultynck G, Leybaert L. 2013b. Paracrine signaling through plasma membrane hemichannels. Biochim Biophys Acta 1828:35–50.

Wei H, Deng F, Chen Y, Qin Y, Hao Y, Guo X. 2014. Ultrafine carbon black induces glutamate and ATP release by activating connexin and pannexin hemichannels in cultured astrocytes. Toxicology 323:32–41.